TRIM29 negatively regulates p53 via inhibition of Tip60

Takuya Sho [a,b], Tsukiyama Tadasuke [a], Tomonobu Sato [a], Takeshi Kondo [b], Jun Cheng [c], Takashi Saku [c], Masahiro Asaka [b] and Shigetsugu Hatakeyama [a,*]

[a] *Department of Biochemistry, Hokkaido University Graduate School of Medicine, Sapporo, Hokkaido 060-8638, Japan*

[b] *Department of Gastroenterology and Hematology, Hokkaido University Graduate School of Medicine, Sapporo 060-8638, Japan*

[c] *Division of Oral Pathology, Department of Tissue Regeneration and Reconstruction, Niigata University Graduate School of Medical and Dental Sciences, Niigata 951-8514, Japan*

* Corresponding author: Shigetsugu Hatakeyama, Department of Biochemistry, Hokkaido University Graduate School of Medicine, N15, W7, Kita-ku, Sapporo, Hokkaido 060-8638, Japan. Tel.: +81 11 706 5899; fax: +81 11 706 5169.

E-mail address: hatas@med.hokudai.ac.jp (S. Hatakeyama)

Key words: TRIM29, p53, Tip60, ubiquitin, ataxia-telangiectasia

Abstract

Ataxia-telangiectasia (AT) is an autosomal recessive genetic disease characterized by immunological deficiencies, neurological degeneration, developmental abnormalities and an increased risk of cancer. Ataxia-telangiectasia group D (ATDC) was initially described as a gene related to AT. ATDC, also known as TRIM29, is structually a member of the tripartite motif (TRIM) family of proteins, some of which have been reported to be highly expressed in some human carcinomas, but the involvement of TRIM29 in carcinogenesis has not been fully elucidated. In this study, we found by using yeast two-hybrid screening that TRIM29 binds to Tip60, which has been reported as a cellular acetyltransferase protein. Overexpression of TRIM29 promoted degradation and changed localization of Tip60 and reduced acetylation of p53 at lysine 120 by Tip60, resulting in enhancement of cell growth and transforming activity. In addition, we found that TRIM29 suppresses apoptosis induced by UV irradiation in HCT116 cell lines. These findings suggest that TRIM29 functions as an oncogene that promotes tumor growth.

1. Introduction

Ataxia-telangiectasia (AT) group D (ATDC) has been reported as one of the suppressive genes responsible for the genetic disorder ataxia-telangiectasia (AT) [1]. AT is a human autosomal recessive genetic disease characterized by immunological deficiencies, neurological degeneration, developmental abnormalities and an increased risk of cancer. Cells isolated from AT patients show hypersensitivity to ionizing radiation, radio-resistant DNA synthesis, elevated recombination, cell cycle abnormalities and aberrant cytoskeletal organization [2].

The *ATDC* gene is located at chromosome 11q23 and encodes a 588 amino acid protein. ATDC protein has been reported to be a member of the tripartite motif (TRIM) protein family with multiple zinc-finger motifs and an adjacent leucine-zipper motif that may allow ATDC to form homo- or heterodimers [1]. Therefore, ATDC is also known as TRIM29, which a member of the tripartite motif (TRIM) family. TRIM proteins have a series of conserved domains, which include a RING, a B box type 1 (B1) and B box type 2 (B2), and a coiled-coil (CC) region [3]. While almost all TRIM proteins have these domains, ATDC contains the B1-B2-CC domains but lacks the RING domain. Several TRIM family members are involved in various cellular processes such as transcriptional regulation, cell growth, apoptosis, development and oncogenesis [4]. So far, it has been reported that TRIM proteins including TRIM19/promyelocytic leukemia protein (PML), TRIM24/transcriptional intermediary factor 1α (TIF1α) and TRIM27/RET finger protein (RFP) have oncogenic activities as a result of chromosomal translocations [5-7].

Though it has been reported that TRIM29 appears to be localized primarily to the

cytoplasm, the function of TRIM29 in physiologic or pathologic processes has not been fully elucidated. TRIM29 has been reported to be overexpressed in lung, bladder, colorectal, ovarian and endometrial cancers and in multiple myeloma. Furthermore, a recent study has shown correlations of ATDC expression in gastric cancer with poor histological grade, large tumor size, great extent of tumor invasion and lymph node metastasis.

Tat-interactive protein 60 (Tip60) was originally identified as a cellular acetyltransferase protein that interacts with Tat derived from human immunodeficiency virus-1 (HIV-1) [8]. Tip60 has divergent functions for many processes such as cellular signaling, DNA damage repair, cell cycle, checkpoint control and apoptosis [9]. Tip60 is a tightly regulated transcriptional coregulator [10, 11], acting in a large multiprotein complex for a range of transcription factors including androgen receptor, Myc, STAT3, NF-κB, E2F1 and p53 [12-17]. Tip60 likely plays an important role in the p53 pathway [18], but the mechanism by which Tip60 acts on p53 has not been elucidated. Tip60 can acetylate p53 on lysine 120 (K120), which is localized within the DNA-binding domain of p53. This domain, in which mutations are often found in human cancer, is an important region for posttranslational modification of p53, followed by the regulation for transcription or apoptosis. A conservative non-acetylated mutant of K120 is defective for apoptosis induction and activation of p53 proapoptotic target genes (*Bax* and *Puma*). However, acetylation of K120 in p53 affects proapoptotic promoters but does not regulate the promoter of p21 [19, 20].

In this study, with the aim of elucidating the molecular function of TRIM29 in carcinogenesis, we identified Tip60 as a novel TRIM29-binding protein by using yeast two-hybrid screening. TRIM29 reduced the acetylation of p53-K120 via change in the

localization and/or degradation of Tip60. We also found that overexpression of TRIM29 promoted cell growth and transforming activity. Moreover, we found that TRIM29 suppressed apoptosis induced by UV irradiation in HCT116 cell lines. These findings may provide evidence for the importance of TRIM29 in carcinogenesis.

2. Materials and methods

2.1. Cell culture

HEK293T and HCT116 cell lines were cultured under an atmosphere of 5% CO_2 at 37°C in DMEM (Sigma, St. Louis, MO) supplemented with 10% fetal bovine serum (Invitrogen, Carlsbad, CA). NIH 3T3 cells lines were cultured under the same conditions in DMEM supplemented with 10% calf serum (CS, Camblex, Walkersville, MD). ACC3 cells were cultured under the same conditions in RPMI1640 supplemented with 10% FBS. The proteasome inhibitor LLnN was purchased from Roche (Branchburg, NJ).

2.2. Cloning of cDNAs and plasmid construction

Human TRIM29 cDNAs were amplified from HeLa cDNA by PCR with BlendTaq (Takara, Tokyo, Japan) using the following primers: 5'-GCGATGGAAGCTGCAGATGCCTCC-3' (TRIM29-sense) and 5'-AGCTCATGGGGCTTCGTTGGACCC-3' (TRIM29-antisense). The amplified fragments were subcloned into pBluescript II SK^+ (Stratagene, La Jolla, CA). FLAG-tagged TRIM29 cDNA was then subcloned into pCR (Invitrogen) for expression in eukaryotic cells. pBTM116 and pACT2 (Clontech Laboratories, Inc. Mountain View, CA) were used for a yeast two-hybrid system. Human Tip60 cDNA was kindly provided by Dr. Ikura (Tohoku University).

2.3. Yeast two-hybrid screening

Complementary DNA encoding the full-length of human TRIM29 was fused in-frame to the nucleotide sequence for the LexA domain (BD) in the yeast two-hybrid vector pBTM116. To screen proteins that interact with TRIM29, we transformed yeast strain L40 (Invitrogen) stably expressing the corresponding pBTM116 vector with a human HeLa cDNA library (Clontech).

2.4. Transfection, immunoprecipitation, and immunoblot analysis

HEK293T cells were transfected by the calcium phosphate method and lysed in a solution containing 50 mmol/L Tris-HCl (pH 7.4), 150 mmol/L NaCl, 1% Nonidet P-40, leupeptin (10 μg/mL), 1 mmol/L phenylmethylsulfonyl fluoride, 400 μmol/L Na_3VO_4, 400 μmol/L EDTA, 10 mmol/L NaF, and 10 mmol/L sodium pyrophosphate. The cell lysates were centrifuged at 16,000 x *g* for 10 min at 4°C, and the resulting supernatant was incubated with antibodies for 2 h at 4°C. Protein A-sepharose (Amersham Pharmacia Biotech Inc, Piscataway, NJ) that had been equilibrated with the same solution was added to the mixture, which was then rotated for 1 h at 4°C. The resin was separated by centrifugation, washed five times with ice-cold lysis buffer, and then boiled in SDS sample buffer. Immunoblot analysis was performed with the following primary antibodies: anti-FLAG (1 μg/mL; M2 or M5, Sigma), anti-HA (1 μg/mL; HA.11/16B12, Covance, Berkeley, CA), anti-HA (1 μg/mL; Y11, Santa Cruz Biotechnology, Santa Cruz, CA), anti-TRIM29 (1:1,000 dilution, IMGENEX, San Diego, USA), anti-β-actin (1 μg/mL; AC15, Sigma), anti-GAPDH (1 μg/mL; 6C5,

Applied Biosystems, Foster City, CA), anti-Tip60 (1:1,000 dilution, AmProx, Carlsbad, CA) and anti-Tip60 (1:1,000, Calbiochem, San Diego, CA). Immune complexes were detected with horseradish peroxidase–conjugated antibodies to mouse or rabbit IgG (1:10,000 dilution, Promega, Madison, WI) and an enhanced chemiluminescence system (Amersham).

2.5. Immunofluorescent staining

HeLa cells expressing FLAG-TRIM29 or HA-Tip60 grown on a glass cover were fixed for 20 min at room temperature with 4% formaldehyde in PBS and then incubated for 1 h at room temperature with primary antibodies to FLAG or HA in PBS containing 0.1% bovine serum albumin and 0.1% saponin. They were then incubated with Alexa546-labeled goat polyclonal antibodies to mouse immunoglobulin or Alexa488-labeled goat polyclonal antibodies to rabbit immunoglobulin (Invitrogen) at a dilution of 1:2,000. The cells were covered with a drop of GEL/MOUNT (Biomeda, Foster City, CA) and then photographed with a CCD camera (DP71, Olympus, Tokyo, Japan) attached to an Olympus BX51 microscope.

2.6. Retroviral infection

Retroviral expression vectors for TRIM29 and c-Src(Y527F) were constructed with pMX-puro and pMX-hyg, respectively. Retroviral expression vectors were kindly provided by Dr. Kitamura (University of Tokyo) [21]. For retrovirus-mediated gene expression, NIH 3T3 cells were infected with retroviruses produced by Plat-E packaging

cells and then cultured in the presence of puromycin (2 μg/mL, Sigma) or hygromycin B (0.2 mg/mL, Sigma). HCT116 cells were infected with retroviruses produced by Plat-A packaging cells and then cultured in the presence of puromycin (0.5 μg/mL) .

2.7. Exposure to UVC

For single exposure of HCT116 cells in a monolayer to UVC, 2×10^5 cells were seeded in a 6-cm dish two days before exposure. The cells were washed with phosphate-buffered saline (PBS) and exposed to UVC (λ=254nm) at different doses from 20 to 80 J/cm^2 (UV crosslinker, Funakoshi, Japan).

2.8. In vivo p53 acetylation assay

The human colon cancer cell line HCT116 was treated with UV as DNA damage. The cells were then incubated for 12 h to induce acetylation of p53 in the presence of an inhibitor of deacetylase, trichostatin (0.5 μM). Cell lysates were immunoprecipitaed with anti-p53 antibody (Clone DO-1, sc-126, Santa Cruz) and then immunoblot analysis was performed with anti-K120-acetylated p53 (AcK120-p53) (10E5, Taipei City, Taiwan).

2.9. RNA interference

Small interfering RNA (siRNA) oligonucleotide sequences specific for human TRIM29 and p53 mRNA were designed by Silencer Predesigned siRNA (Ambion,

Foster City, CA). pSUPER.retro.puro. vectors (OligoEngine, Seattle, WA) containing shRNAs were infected into ACC3 or HCT116 cells. After 24 h, the resulting cell lines were used for immunoblot analysis to detect the expression level of TRIM29.

2.10. Cell proliferation assay

HCT116 cells in which TRIM29 or an empty vector (Mock) was stably expressed by using a retroviral expression system were seeded in 10-cm dishes (3×10^4 cells) and harvested for determination of cell number at indicated times.

2.11. Focus formation assay

NIH 3T3 cell lines stably expressing FLAG-TRIM29 and/or c-Src(Y527F) were plated at a density of 1×10^4 cells in 60-mm dishes with drug selection. After 2 weeks, confluent cells on dishes were stained by crystal violet and focus formation was observed under a microscope.

2.12. Colony formation assay

For the colony formation assay, 1×10^5 cells were plated in 60-mm dishes containing 0.4% soft agar and cultured for 2 weeks. The numbers of colonies with a diameter of >0.125 mm in randomized areas (1 cm^2) were counted.

2.13. Apoptosis assay

Assessment of apoptosis was performed by measurement of the intensity of the sub-G_1 peak. For the sub-G_1 peak, HCT116 cells were incubated with or without UV irradiation (10-80 J/m^2) for 18 and 24 h. The cells were treated with propidium iodide and then the sub-G_1 peak was analyzed with a FACSCalibur flow cytometer (Becton Dickinson, San Jose, CA).

2.14. Statistical analysis

The unpaired Student's *t* test was used to determine the statistical significance of experimental data.

3. Results

3.1. TRIM29 interacts with and mediates degradation of Tip60

To identify proteins that interact with TRIM29, we screened a pACT2 HeLa cDNA library with pBTM116-hTRIM29 plasmid as a bait by using a yeast two-hybrid system. We obtained 60 grown clones from 1.25×10^6 transformants in selection medium. Finally, we obtained two positive clones that may interact with TRIM29 in this screening: Tip60 and Xab2. Interaction between TRIM29 and Tip60 was again confirmed by a β-galactosidase assay (Fig. 1A). To examine whether TRIM29 physically interacts with Tip60 in mammalian cells, we performed an in vivo binding assay using cells transfected with expression vectors. We expressed FLAG-TRIM29 together with HA-Tip60 in HEK293T cells. Cell lysates were subjected to immunoprecipitation with an antibody to HA, and the resulting precipitates were subjected to immunoblot analysis with an antibody to FLAG. FLAG-TRIM29 was co-precipitated by the antibody to HA, indicating that TRIM29 specifically interacts with Tip60 (Fig. 1B). To further confirm the interaction between endogenous Tip60 and FLAG-TRIM29, we performed an in vivo binding assay using cells transfected with an expression vector encoding FLAG-TRIM29. Immunoblot analysis showed that FLAG-TRIM29 was co-precipitated by the antibody to Tip60, indicating that TRIM29 specifically interacts with Tip60 (Fig. 1C).

It has been reported that some TRIM family proteins form homodimers or heterodimers. There is a possibility that even though TRIM29 has no RING-finger domain, TRIM29 interacts with other TRIM family proteins with a RING-finger domain

and affects the stability of Tip60. To examine whether TRIM29 ubiquitinates Tip60, we performed an in vivo ubiquitination assay. However, overexpression of TRIM29 did not enhance polyubiquitination of HA-Tip60 (data not shown). We further examined the effect of TRIM29 on the degradation of endogenous Tip60 in vivo. Immunoblot analysis showed that overexpression of TRIM29 attenuated the expression of endogenous Tip60 in a TRIM29 dose-dependent manner (Fig. 1D). To determine whether the decrease in expression level of Tip60 is enhanced by proteasome-dependent degradation, we performed immunobolot analysis with anti-Tip60 antibody using cell lysates incubated with the proteasome inhibitor LLnL. Immunoblot analysis showed that the proteasome inhibitor LLnL inhibited the degradation of Tip60, suggesting that degradation of Tip60 by TRIM29 is dependent on proteasome activity (Fig. 1E).

3.2. TRIM29 colocalizes with Tip60

We investigated the effect of TRIM29 on subcellular localization of Tip60. To test each localization, we performed immunofluorescent staining of TRIM29 and Tip60. We transiently transfected FLAG-TRIM29 and HA-Tip60 expression vectors into HeLa cells and stained the cells by using anti-FLAG and anti-HA antibodies. Tip60 was usually expressed in the nucleus, whereas TRIM29 was expressed in the cytosol. Overexpression of TRIM29 caused a decrease in nuclear staining of Tip60 and an increase in localization of Tip60 in the cytosol (Fig. 2). Similar results were obtained by using COS7 cells (data not shown). These findings suggest that TRIM29 regulates Tip60 localization and then TRIM29 affects the physiological function of Tip60.

3.3. TRIM29 reduces acetylation of p53 at K120 by Tip60

Lysine (K) 120 is located in the L1 loop of the DNA-binding core domain of p53 and is conserved in all known species which encode p53 including humans, mice, *D. melanogaster* and *C. elegans*, suggesting a critical role for this residue in p53 function [20]. Tumor-associated gene mutations of K120 have often been observed in several different types of human cancer [19, 22]. Furthermore, it has been reported that Tip60 induces its acetylation specifically at K120 in the DNA-binding domain and is required for both cell growth arrest and apoptosis mediated by p53 [20]. Taken together, K120 acetylation by Tip60 is crucial for p53-dependent apoptosis. To determine the condition of DNA damage response to induce Tip60-mediated p53 acetylation, we performed immunoblot analysis using an antibody specific to K120-acetylated p53 (AcK120-p53) with the human colorectal carcinoma cell line HCT116 damaged by UV irradiation. Twenty hours after exposure to UV light (20-80 J/m^2), whole-cell extracts at each UV dose were immunoprecipitated with anti-p53 antibody and then immunoblotted with antibodies specific for AcK120-p53. Immunoblot analysis showed that UV-mediated DNA damage induces acetylation of p53 at K120 (Fig. 3A).

Next, to elucidate the role of TRIM29 in DNA damage-induced p53 activation by Tip60, we tested whether TRIM29 affects K120 acetylation of endogenous p53. Twenty hours after exposure to UV light (80 J/m^2), HCT116 cells stably expressing TRIM29 or an empty vector (Mock) were harvested and the acetylation of p53 was analyzed. Immunoblot analysis showed that HCT116 cells stably expressing TRIM29 had no obvious difference in p53 accumulation upon DNA damage compared to Mock cells but had significantly reduced levels of acetylated p53 at K120 (Fig. 3B). These results

suggest that TRIM29 reduces acetylation of p53 at K120 by Tip60.

3.4. TRIM29 suppresses apoptosis induced by UV

Given that TRIM29 causes a decrease in Tip60-mediated acetylation of p53 at K120, overexpression of TRIM29 may inhibit p53-dependent apoptosis by UV treatment. We analyzed the susceptibility to UV-mediated DNA damage using the HCT116 cell line infected with a retrovirus encoding FLAG-TRIM29 or the corresponding empty vector (Mock). The resulting cell lines were treated with UV, incubated for 24 h, and stained with propidium iodide (PI), and the sub-G1 peak was measured by a flowcytomer to detect apoptotic cells according to DNA content. Flowcytometric analysis showed that approximately 37.4% of Mock cells were apoptotic cells, whereas only 11.1% of TRIM29-expressing cells were counted as apoptotic cells after 24-h UV treatment by flowcytometric analysis (Fig. 4A and B). Next, we performed an apoptosis assay using low doses of UV (10 and 20 J/m^2). The apoptosis assay showed that overexpression of TRIM29 also suppressed apoptosis induced by low doses of UV (10 and 20 J/m^2), suggesting that TRIM29 plays a physiological role in protection against UV irradiation (Fig. 4C). To clarify the relationship between TRIM29 and p53 in UV-induced apoptosis, p53-knock down cells (HCT116.p53kd) were used for a UV-mediated apoptosis assay. The HCT116 cell line in which p53 was knocked down was further transfected with an expression vector encoding TRIM29 (HCT116.p53kd.TRIM29) (Fig. 4D). We performed an apoptosis assay using these cell lines. UV-induced apoptosis was inhibited in HCT116.p53kd cells compared with mock. UV-induced apoptosis in HCT116.p53kd.TRIM29 was almost the

same as apoptosis in HCT116.p53kd cells and apoptosis in HCT116.TRIM29, indicating that UV-induced apoptosis in HCT116.p53kd is not increased by overexpression of TRIM29 (Fig. 4E). These findings suggest that TRIM29 does not function as a regulator of an apoptotic pathway other than the p53-mediated apoptotic pathway.

3.5. TRIM29 affects cell growth and anchorage-independent growth

It has been reported that overexpression of TRIM29 promotes cell growth of the osteosarcoma cell line Saos-2 and the breast cancer cell line BT-549 [23]. We further confirmed the effect of TRIM29 on cell growth using HCT116 cells. HCT116 cells overexpressing FLAG-TRIM29 or an empty vector (Mock) were seeded and cell numbers were counted at indicated times. Overexpression of TRIM29 significantly increased the growth rate compared with that of Mock (Fig. 5A). Next, to determine whether TRIM29 affects cell transformation by the active form of c-Src (c-Src(Y527F)), we established an NIH 3T3 cell line stably expressing the active form of c-Src(Y527F) by retroviral infection. The resulting cell line was further infected with recombinant retroviruses encoding FLAG-TRIM29 (Fig. 5B). The effect of TRIM29 on cell proliferation was confirmed by focus formation assays using these cell lines. Many foci were formed by the NIH 3T3 cell line expressing c-Src(Y527F), and the NIH 3T3 cell line expressing both c-Src(Y527F) and TRIM29 formed more foci, suggesting that TRIM29 enhances the transformation by oncogenic activity of c-Src(Y527F) (Fig. 5C). The ability of these NIH 3T3 cell lines to form colonies in soft agar was also analyzed to evaluate their ability to undergo anchorage-independent growth. Cells that had not

been infected c-Src(Y527F) formed few colonies, whereas cells expressing c-Src(Y527F) formed many colonies. The combination of c-Src(Y527F) and TRIM29 increased the ability for anchorage-independent growth (Fig. 5D and E). These findings suggest that TRIM29 functions as a positive regulator for anchorage-independent growth.

3.6. Knockdown of TRIM29 expression causes cell morphological changes followed by apoptosis

To knock down endogenous TRIM29, we introduced shRNA specific for human TRIM29 (sh-1, sh-2, sh-3) or non-targeting shRNA as a control (sh-control) into the ACC3 cell line in which TRIM29 is highly expressed. The HCT116 cell line was used as a negative control because we confirmed that TRIM29 is not expressed in HCT116 cells (Fig. 6A). Immunoblot analysis showed that the expression level of TRIM29 was reduced by shRNA for TRIM29 (sh-2 and sh-3). In contrast, TRIM29 protein levels were not significantly decreased in cells infected with sh-1 (Fig. 6B). The shRNA for TRIM29 (sh-2 and sh-3) caused morphological changes, including rounding of cell shapes and decrease in size, and detachment from the dish, consistent with phenomena often observed in apoptosis (Fig. 6C). The HCT116 cell line was used as a negative control because we have already confirmed that TRIM29 is not expressed in HCT116 cells. Similar effects were not observed using HCT116 cells. These findings suggest that TRIM29 is required for cell viability for TRIM29-expressing cells and that TRIM29 functions as a positive regulator for cell growth.

4. Discussion

Our studies demonstrate a functional role of TRIM29 in human tumorigenesis. TRIM29 has been reported to be overexpressed in lung, bladder, colorectal, ovarian, gastric, pancreatic and endometrial cancers and in multiple myeloma [24-32]. Interestingly, opposite results were obtained in melanoma and in breast, head and neck, and prostate cancers [33-38]. The significance of such a paradoxical pattern of TRIM29 expression in cancer may suggest that the function of TRIM29 is dependent on cellular or tissue context. Recently, it has been reported that TRIM29 is highly expressed in gastric cancer with poor histological grade, larger tumor size, greater extent of tumor invasion and lymph node metastasis [29]. TRIM29 may thus play a pivotal role in differentiation, proliferation, and progression of gastric cancer cells. Taken together, it is important to unveil the molecular mechanism for regulation of the expression level of TRIM29 and furthermore to analyze gene mutation or single nucleotide polymorphisms of the *TRIM29* gene using several cancer tissues or cancer cell lines in the future.

Several recent reports have shown the role of TRIM29 in tumorigenesis examined on the basis of functional studies. A recent report has shown that TRIM29 is an important positive regulator of β-catenin-dependent signaling in pancreatic cancer [30]. In normal pancreatic cells lacking TRIM29, Disheveled-2 (Dvl-2) is localized in the cytoplasm and is not bound to the axin/glycogen synthase kinase 3β (GSK-3β)/APC complex, which degrades and ubiquitinates phosphorylated β-catenin and targets it for ubiquitin-mediated degradation. In pancreatic cancer cells expressing high levels of TRIM29, TRIM29 binds to and stabilizes Dvl-2, resulting in the release of β-catenin from the destruction complex, increased β-catenin levels, and subsequent activation of

downstream β-catenin/TCF-regulated target genes. Thus, TRIM29 likely stabilizes β-catenin via inhibition of Dvl-2, a negative regulator of GSK-3β in Wnt/β-catenin signaling. This report showed one of the functional roles of TRIM29 in human tumorigenesis and indicated the possibility of TRIM29 being a potential therapeutic target in pancreatic cancer.

Ionizing irradiation induced apoptosis to a greater extent in AT5BIVA cells and ATDC partially suppressed this irradiation-induced apoptosis. It has been reported that ATDC increases cell proliferation via inhibition of p53 nuclear activities [40]. The association of p53 and ATDC results in p53 sequestration outside the nucleus. These results provide novel mechanistic insights into the function of ATDC and offer an explanation for how ATDC promotes cancer cell proliferation. We also demonstrated that *TRIM29* functions as an oncogene as revealed by results of a cell proliferation assay, focus formation assay and colony formation assay in our study.

Others have reported that the amount of TRIM29 increased in keratinocytes after exposure to UVB and that knock-down of TRIM29 by short-hairpin RNA interference decreases the viability of keratinocytes after UVB exposure, suggesting that TRIM29 participates in the survival of differentiating keratinocytes that are exposed to UVB and pro-death stimuli [41]. We also showed that knock-down of TRIM29 with shRNA causes morphological changes of ACC3 cells in which apoptosis is likely to be induced.

We found that TRIM29 interacts with one of the MYST family acetyltransferases, Tip60, and that overexpression of TRIM29 attenuated expression of endogenous Tip60 in a TRIM29 dose-dependent manner. We could not find that overexpression of TRIM29 enhances polyubiquitination of Tip60. However, overexpression of TRIM29 caused a decrease in nuclear staining of Tip60. These findings suggest that TRIM29

affects the stability of Tip60 via subcellular translocation from the nucleus to the cytosol.

Many recent studies have shown the role for Tip60 in tumorigenesis. Tip60 causes UV-induced transcription of several p53 targets. Post-translational modification of the DNA-binding domain of p53 including acetylation of K120 occurs rapidly after DNA damage and its acetylation is catalyzed by Tip60. Tip60 is required for both cell growth arrest and apoptosis mediated by p53 [39]. Interestingly, this modification is crucial for p53-dependent apoptosis but is dispensable for its mediated growth arrest. Mutation of lysine 120 to arginine, which occurs in human cancer, and the corresponding acetylation-defective tumor mutant (K120R) abrogates p53-mediated apoptosis but not growth arrest. K120R mutation selectively blocks transcription of pro-apoptotic target genes such as *Bax* and *Puma*, while the non-apoptotic targets *p21* and *MDM2* remain unaffected. Consistent with this, depletion of Tip60 inhibits the ability of p53 to activate *Bax* and *Puma* transcription [19, 20]. Actually, in this study, we demonstrated that overexpression of TRIM29 reduces acetylation of p53 at K120 by Tip60 and suppresses apoptosis induced by UV irradiation, suggesting that TRIM29 functions as a negative regulator of p53 via inhibition of Tip60-mediated acetylation.

In conclusion, our observations indicate that TRIM29 is a positive mediator affecting tumor growth, apoptosis, and resistance to UV irradiation, and results of further studies on TRIM29 may be useful for establishing new therapies for cancers, immunological deficiencies, and neurological degeneration accompanying AT. Moreover, analysis by a genetic approach using transgenic or knock-out mice is needed to clarify physiological functions of TRIM29.

Acknowledgments

We would like to thank Drs. T. Kitamura and T. Ikura for the plasmids and Y. Soida for help in preparing the manuscript.

This work was supported in part by a research grant from Grant-in-Aid for Scientific Research on Priority Areas from the Ministry of Education, Culture, Sports, Science and Technology, Ono Cancer Research Fund, The Ichiro Kanehara Foundation, The Nakatomi Foundation, Japan Brain Foundation and the Research Foundation Ituu Laboratory (to S. Hatakeyama).

References

[1] L.N. Kapp, R.B. Painter, L.C. Yu, N. van Loon, C.W. Richard, 3rd, M.R. James, D.R. Cox, J.P. Murnane, Cloning of a candidate gene for ataxia-telangiectasia group D, Am J Hum Genet 51 (1992) 45-54.

[2] P.M. Brzoska, H. Chen, Y. Zhu, N.A. Levin, M.H. Disatnik, D. Mochly-Rosen, J.P. Murnane, M.F. Christman, The product of the ataxia-telangiectasia group D complementing gene, ATDC, interacts with a protein kinase C substrate and inhibitor, Proc Natl Acad Sci USA 92 (1995) 7824-7828.

[3] A. Reymond, G. Meroni, A. Fantozzi, G. Merla, S. Cairo, L. Luzi, D. Riganelli, E. Zanaria, S. Messali, S. Cainarca, A. Guffanti, S. Minucci, P.G. Pelicci, A. Ballabio, The tripartite motif family identifies cell compartments, EMBO J 20 (2001) 2140-2151.

[4] N.A. Quaderi, S. Schweiger, K. Gaudenz, B. Franco, E.I. Rugarli, W. Berger, G.J. Feldman, M. Volta, G. Andolfi, S. Gilgenkrantz, R.W. Marion, R.C. Hennekam, J.M. Opitz, M. Muenke, H.H. Ropers, A. Ballabio, Opitz G/BBB syndrome, a defect of midline development, is due to mutations in a new RING finger gene on Xp22, Nat Genet 17 (1997) 285-291.

[5] K. Jensen, C. Shiels, P.S. Freemont, PML protein isoforms and the RBCC/TRIM motif, Oncogene 20 (2001) 7223-7233.

[6] E. Remboutsika, Y. Lutz, A. Gansmuller, J.L. Vonesch, R. Losson, P. Chambon, The putative nuclear receptor mediator TIF1alpha is tightly associated with euchromatin, J Cell Sci 112 (Pt 11) (1999) 1671-1683.

[7] S.H. Dho, K.S. Kwon, The Ret finger protein induces apoptosis via its RING

finger-B box-coiled-coil motif, J Biol Chem 278 (2003) 31902-31908.

[8] J. Kamine, B. Elangovan, T. Subramanian, D. Coleman, G. Chinnadurai, Identification of a cellular protein that specifically interacts with the essential cysteine region of the HIV-1 Tat transactivator, Virology 216 (1996) 357-366.

[9] T. Ikura, V.V. Ogryzko, M. Grigoriev, R. Groisman, J. Wang, M. Horikoshi, R. Scully, J. Qin, Y. Nakatani, Involvement of the TIP60 histone acetylase complex in DNA repair and apoptosis, Cell 102 (2000) 463-473.

[10] V. Sapountzi, I.R. Logan, C.N. Robson, Cellular functions of TIP60, Int J Biochem Cell Biol 38 (2006) 1496-1509.

[11] M. Squatrito, C. Gorrini, B. Amati, Tip60 in DNA damage response and growth control: many tricks in one HAT, Trends Cell Biol 16 (2006) 433-442.

[12] L. Gaughan, M.E. Brady, S. Cook, D.E. Neal, C.N. Robson, Tip60 is a co-activator specific for class I nuclear hormone receptors, J Biol Chem 276 (2001) 46841-46848.

[13] S.R. Frank, T. Parisi, S. Taubert, P. Fernandez, M. Fuchs, H.M. Chan, D.M. Livingston, B. Amati, MYC recruits the TIP60 histone acetyltransferase complex to chromatin, EMBO Rep 4 (2003) 575-580.

[14] H. Xiao, J. Chung, H.Y. Kao, Y.C. Yang, Tip60 is a co-repressor for STAT3, J Biol Chem 278 (2003) 11197-11204.

[15] J.H. Kim, B. Kim, L. Cai, H.J. Choi, K.A. Ohgi, C. Tran, C. Chen, C.H. Chung, O. Huber, D.W. Rose, C.L. Sawyers, M.G. Rosenfeld, S.H. Baek, Transcriptional regulation of a metastasis suppressor gene by Tip60 and beta-catenin complexes, Nature 434 (2005) 921-926.

[16] S. Taubert, C. Gorrini, S.R. Frank, T. Parisi, M. Fuchs, H.M. Chan, D.M.

Livingston, B. Amati, E2F-dependent histone acetylation and recruitment of the Tip60 acetyltransferase complex to chromatin in late G1, Mol Cell Biol 24 (2004) 4546-4556.

[17] G. Legube, L.K. Linares, S. Tyteca, C. Caron, M. Scheffner, M. Chevillard-Briet, D. Trouche, Role of the histone acetyl transferase Tip60 in the p53 pathway, J Biol Chem 279 (2004) 44825-44833.

[18] G. Legube, L.K. Linares, C. Lemercier, M. Scheffner, S. Khochbin, D. Trouche, Tip60 is targeted to proteasome-mediated degradation by Mdm2 and accumulates after UV irradiation, EMBO J 21 (2002) 1704-1712.

[19] S.M. Sykes, H.S. Mellert, M.A. Holbert, K. Li, R. Marmorstein, W.S. Lane, S.B. McMahon, Acetylation of the p53 DNA-binding domain regulates apoptosis induction, Mol Cell 24 (2006) 841-851.

[20] Y. Tang, J. Luo, W. Zhang, W. Gu, Tip60-dependent acetylation of p53 modulates the decision between cell-cycle arrest and apoptosis, Mol Cell 24 (2006) 827-839.

[21] S. Morita, T. Kojima, T. Kitamura, Plat-E: an efficient and stable system for transient packaging of retroviruses, Gene Ther 7 (2000) 1063-1066.

[22] H. Deissler, A. Kafka, E. Schuster, G. Sauer, R. Kreienberg, R. Zeillinger, Spectrum of p53 mutations in biopsies from breast cancer patients selected for preoperative chemotherapy analysed by the functional yeast assay to predict therapeutic response, Oncol Rep 11 (2004) 1281-1286.

[23] Y. Hosoi, L.N. Kapp, J.P. Murnane, Y. Matsumoto, A. Enomoto, T. Ono, K. Miyagawa, Suppression of anchorage-independent growth by expression of the ataxia-telangiectasia group D complementing gene, ATDC, Biochem Biophys

Res Commun 348 (2006) 728-734.

[24] L. Hawthorn, L. Stein, J. Panzarella, G.M. Loewen, H. Baumann, Characterization of cell-type specific profiles in tissues and isolated cells from squamous cell carcinomas of the lung, Lung Cancer 53 (2006) 129-142.

[25] L. Dyrskjot, M. Kruhoffer, T. Thykjaer, N. Marcussen, J.L. Jensen, K. Moller, T.F. Orntoft, Gene expression in the urinary bladder: a common carcinoma in situ gene expression signature exists disregarding histopathological classification, Cancer Res 64 (2004) 4040-4048.

[26] O.K. Glebov, L.M. Rodriguez, P. Soballe, J. DeNobile, J. Cliatt, K. Nakahara, I.R. Kirsch, Gene expression patterns distinguish colonoscopically isolated human aberrant crypt foci from normal colonic mucosa, Cancer Epidemiol Biomarkers Prev 15 (2006) 2253-2262.

[27] T. Ohmachi, F. Tanaka, K. Mimori, H. Inoue, K. Yanaga, M. Mori, Clinical significance of TROP2 expression in colorectal cancer, Clin Cancer Res 12 (2006) 3057-3063.

[28] A.D. Santin, F. Zhan, S. Bellone, M. Palmieri, S. Cane, E. Bignotti, S. Anfossi, M. Gokden, D. Dunn, J.J. Roman, T.J. O'Brien, E. Tian, M.J. Cannon, J. Shaughnessy, Jr., S. Pecorelli, Gene expression profiles in primary ovarian serous papillary tumors and normal ovarian epithelium: identification of candidate molecular markers for ovarian cancer diagnosis and therapy, Int J Cancer 112 (2004) 14-25.

[29] Y. Kosaka, H. Inoue, T. Ohmachi, T. Yokoe, T. Matsumoto, K. Mimori, F. Tanaka, M. Watanabe, M. Mori, Tripartite motif-containing 29 (TRIM29) is a novel marker for lymph node metastasis in gastric cancer, Ann Surg Oncol 14

(2007) 2543-2549.

[30] L. Wang, D.G. Heidt, C.J. Lee, H. Yang, C.D. Logsdon, L. Zhang, E.R. Fearon, M. Ljungman, D.M. Simeone, Oncogenic function of ATDC in pancreatic cancer through Wnt pathway activation and beta-catenin stabilization, Cancer Cell 15 (2009) 207-219.

[31] G.L. Mutter, J.P. Baak, J.T. Fitzgerald, R. Gray, D. Neuberg, G.A. Kust, R. Gentleman, S.R. Gullans, L.J. Wei, M. Wilcox, Global expression changes of constitutive and hormonally regulated genes during endometrial neoplastic transformation, Gynecol Oncol 83 (2001) 177-185.

[32] F. Zhan, J. Hardin, B. Kordsmeier, K. Bumm, M. Zheng, E. Tian, R. Sanderson, Y. Yang, C. Wilson, M. Zangari, E. Anaissie, C. Morris, F. Muwalla, F. van Rhee, A. Fassas, J. Crowley, G. Tricot, B. Barlogie, J. Shaughnessy, Jr., Global gene expression profiling of multiple myeloma, monoclonal gammopathy of undetermined significance, and normal bone marrow plasma cells, Blood 99 (2002) 1745-1757.

[33] A.P. Smith, K. Hoek, D. Becker, Whole-genome expression profiling of the melanoma progression pathway reveals marked molecular differences between nevi/melanoma in situ and advanced-stage melanomas, Cancer Biol Ther 4 (2005) 1018-1029.

[34] M. Nacht, A.T. Ferguson, W. Zhang, J.M. Petroziello, B.P. Cook, Y.H. Gao, S. Maguire, D. Riley, G. Coppola, G.M. Landes, S.L. Madden, S. Sukumar, Combining serial analysis of gene expression and array technologies to identify genes differentially expressed in breast cancer, Cancer Res 59 (1999) 5464-5470.

[35] L. Zhang, C.J. Duan, C. Binkley, G. Li, M.D. Uhler, C.D. Logsdon, D.M. Simeone, A transforming growth factor beta-induced Smad3/Smad4 complex directly activates protein kinase A, Mol Cell Biol 24 (2004) 2169-2180.

[36] E. LaTulippe, J. Satagopan, A. Smith, H. Scher, P. Scardino, V. Reuter, W.L. Gerald, Comprehensive gene expression analysis of prostate cancer reveals distinct transcriptional programs associated with metastatic disease, Cancer Res 62 (2002) 4499-4506.

[37] J. Luo, D.J. Duggan, Y. Chen, J. Sauvageot, C.M. Ewing, M.L. Bittner, J.M. Trent, W.B. Isaacs, Human prostate cancer and benign prostatic hyperplasia: molecular dissection by gene expression profiling, Cancer Res 61 (2001) 4683-4688.

[38] Y.P. Yu, D. Landsittel, L. Jing, J. Nelson, B. Ren, L. Liu, C. McDonald, R. Thomas, R. Dhir, S. Finkelstein, G. Michalopoulos, M. Becich, J.H. Luo, Gene expression alterations in prostate cancer predicting tumor aggression and preceding development of malignancy, J Clin Oncol 22 (2004) 2790-2799.

[39] S. Tyteca, G. Legube, D. Trouche, To die or not to die: a HAT trick, Mol Cell 24 (2006) 807-808.

[40] Z. Yuan, A. Villagra, L. Peng, D. Coppola, M. Glozak, E.M. Sotomayor, J. Chen, W.S. Lane, E. Seto, The ATDC (TRIM29) protein binds p53 and antagonizes p53-mediated functions, Mol Cell Biol 30 (2010) 3004-3015.

[41] V. Bertrand-Vallery, N. Belot, M. Dieu, E. Delaive, N. Ninane, C. Demazy, M. Raes, M. Salmon, Y. Poumay, F. Debacq-Chainiaux, O. Toussaint, Proteomic profiling of human keratinocytes undergoing UVB-induced alternative differentiation reveals TRIpartite motif protein 29 as a survival factor, PLoS

One 5 (2010) e10462.

Figure legends

Fig. 1. TRIM29 interacts with Tip60. (A) Tip60 was isolated by yeast two-hybrid screening using TRIM29 as bait. Interaction of TRIM29 and Tip60 was confirmed by β-galactosidase assay. (B) In vivo binding assay between FLAG-TRIM29 and HA-Tip60. FLAG-TRIM29 and HA-Tip60 expression vectors were transfected into HEK293T cells. Cell lysates (WCL) were immunoprecipitated with anti-HA antibody and immunoblotted with anti-FLAG and anti-HA antibodies. A portion of the cell lysate corresponding to 3% of the input for immunoprecipitation was also subjected to immunoblot analysis (IB). (C) In vivo binding assay between FLAG-TRIM29 and endogenous Tip60. FLAG-TRIM29 vectors were transfected into HEK293T cells. Cell lysates (WCL) were immunoprecipitated with anti-Tip60, anti-FLAG or control antibody and immunoblotted with anti-TRIM29 antibodies. A portion of the cell lysate corresponding to 3% of the input for immunoprecipitation was also subjected to immunoblot analysis (IB). (D) Down-regulation of endogenous Tip60 by exogenous TRIM29. HCT116 cells were transfected with different amounts of FLAG-TRIM29. Cell lysates were then subjected to immunoblot analysis with anti-Tip60, anti-FLAG and anti-β-actin antibodies. (E) Proteasome-dependent degradation of Tip60 by TRIM29. HCT116 cells transfected with an expression vector encoding FLAG-TRIM29 were cultured with LLnL (10 μM) for indicated times. Cell lysates were then subjected to immunoblot analysis with anti-Tip60, anti-FLAG and anti-β-actin antibodies.

Fig. 2. TRIM29 affects subcellular localization of Tip60. HeLa cells were transiently transfected with expression vectors encoding HA-tagged Tip60 and different amounts of

FLAG-tagged TRIM29. Cells were fixed and stained with anti-FLAG and anti-HA antibodies. The green and red colors represent TRIM29 and Tip60, respectively.

Fig. 3. TRIM29 reduces acetylation of p53 at K120 by Tip60. (A) HCT116 cells stably expressing TRIM29 or an empty vector (Mock) were treated with UV (20, 40 or 80 J/m^2) and cultured for 12 h. Cell lysates (WCL) were immunoprecipitated with anti-p53 antibody (DO-1) and immunoblotted with anti-K120-acetylated (AcK120)-p53 antibody. (B) In vivo acetylation of p53 at K120 by Tip60. HCT116 cell lines were treated with or without UV (80 J/m^2) and then cultured for 4 or 8 h. Total cell extracts were immunoprecipitaed with anti-p53 antibody (DO-1) and then immunoblotted using anti-FLAG, anti-Tip60, anti-AcK120-p53 and anti-p53 (DO-1) antibodies.

Fig. 4. TRIM29 suppresses apoptosis induced by UV treatment. (A) Measurement of sub-G_1 peak. HCT116 cell lines were incubated for 0, 12, 18 and 24 h after UV treatment (80 J/m^2). The cells were treated with propidium iodide and then sub-G_1 peaks were analyzed with a FACSCalibur flow cytometer. (B) Quantification of apoptotic cell fraction. Percentages of apoptotic cells at each time in (A) are shown. (C) Inhibition of UV-mediated apoptosis by TRIM29 at a low dose of UV irradiation. HCT116 cell lines were incubated for 18 h after UV treatment (0, 10 or 20 J/m^2). The cells were treated with propidium iodide, and then sub-G_1 peaks were analyzed with a FACSCalibur flow cytometer. Percentages of apoptotic cells at the indicated times are shown. (D) Establishment of cell lines in which FLAG-TRIM29 is overexpressed and p53 is knocked down. HCT116 cells were infected with a retrovirus containing a human p53 short hairpin RNA (shRNA) or mock sequence and then transfected with an

expression vector encoding FLAG-tagged TRIM29. Each expression was checked by immunoblot analysis using anti-53, anti-FLAG and anti-GAPDH antibodies. (E) Effect of UV-mediated apoptosis by TRIM29 and p53. HCT116 cell lines in which p53 is knocked down and/or TRIM29 is overexpresssed were incubated for 18 h after UV treatment (80 J/m^2). The cells were treated with propidium iodide, and then sub-G_1 peaks were analyzed with a FACSCalibur flow cytometer.

Fig. 5. TRIM29 affects cell growth and colony formation activity. (A) Acceleration of cell proliferation by TRIM29. HCT116 cells infected with a retrovirus encoding FLAG-TRIM32 or the corresponding empty vector (Mock) were seeded at 3 x 10^4 cells in six-well plates and harvested for determination of cell number at indicated times. Data are means ± SD of values from three independent experiments. (B) Establishment of cell lines expressing FLAG-TRIM29 and/or c-Src(Y527F). NIH 3T3 cells infected with a retrovirus encoding FLAG-TRIM29 or the corresponding empty vector (Mock). NIH 3T3 cell lines were further infected with a retrovirus for c-Src(Y527F). Each expression was checked by immunoblot analysis using anti-FLAG, anti-Src and anti-β-actin antibodies. (C) Focus formation assay of NIH 3T3 cells infected with retrovirus vectors encoding FLAG-TRIM29 and/or c-Src(Y527F). Cell lines were plated at a density of 1 x 10^4 cells in 60-mm dishes with drug selection. After 2 weeks, confluent cells on dishes were stained by crystal violet and focus formation was observed under a microscope. Scale bar, 0.1 mm. (D) Colony formation assay of NIH 3T3 cells infected with retrovirus vectors encoding FLAG-TRIM29 and/or c-Src(Y527F). NIH 3T3 cell lines were seeded at 1 x 10^5 cells in 60-mm dishes containing 0.4% soft agar and cultured for 2 weeks. Scale bar, 0.1 mm. (E)

Quantification of colony numbers on soft agar. The numbers of colonies with a diameter of more than 0.125 mm in randomized areas (per 1 cm^2) were counted. Data are means ± SD of values from three independent experiments. *P* values for the indicated comparisons were determined by Student's *t*-test.

Fig. 6. Effect of TRIM29 RNAi on cell morphology. (A) Expression of TRIM29 in HCT116 and ACC3 cells. Cell lysates from HCT116 and ACC3 cells were subjected to immunoblot analysis with anti-TRIM29 or anti-β-actin antibody (B) ACC3 cells were transfected with plasmids containing a human TRIM29 short hairpin RNA (shRNA) sequence (sh-1, sh-2 and sh-3) or control shRNA (Mock). At 24 h after transfection, whole cell lysates were analyzed by immunoblotting using anti-TRIM29 and anti-β-actin antibodies. (C) Microscopic analysis of TRIM29 shRNA-infected ACC3 cells. HCT116 cells in which TRIM29 is not expressed were used as negative controls. Seventy-two h after infection with sh-1, sh-2 or sh-3, cells were observed by microscopy.

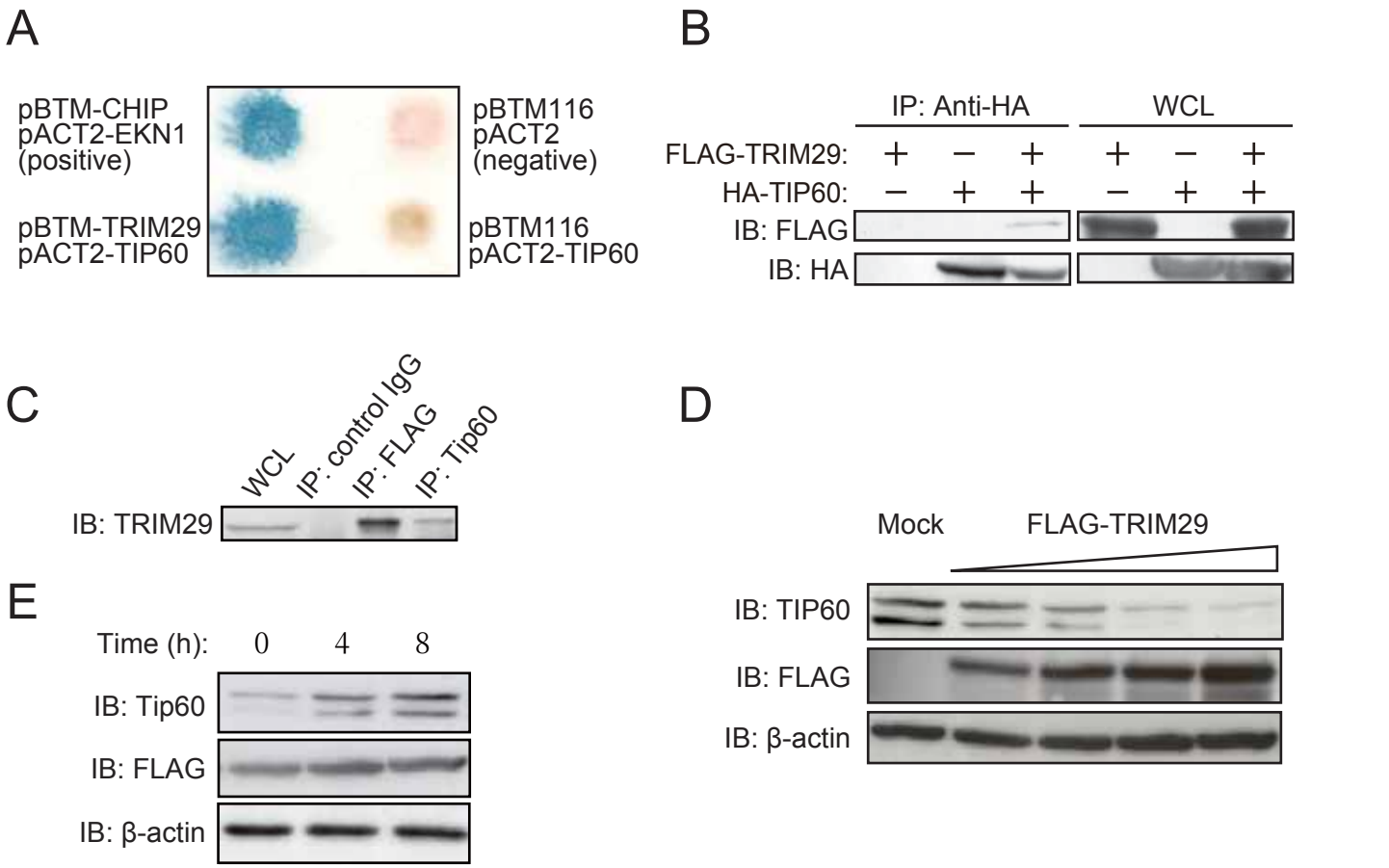

Sho et al. Fig. 1

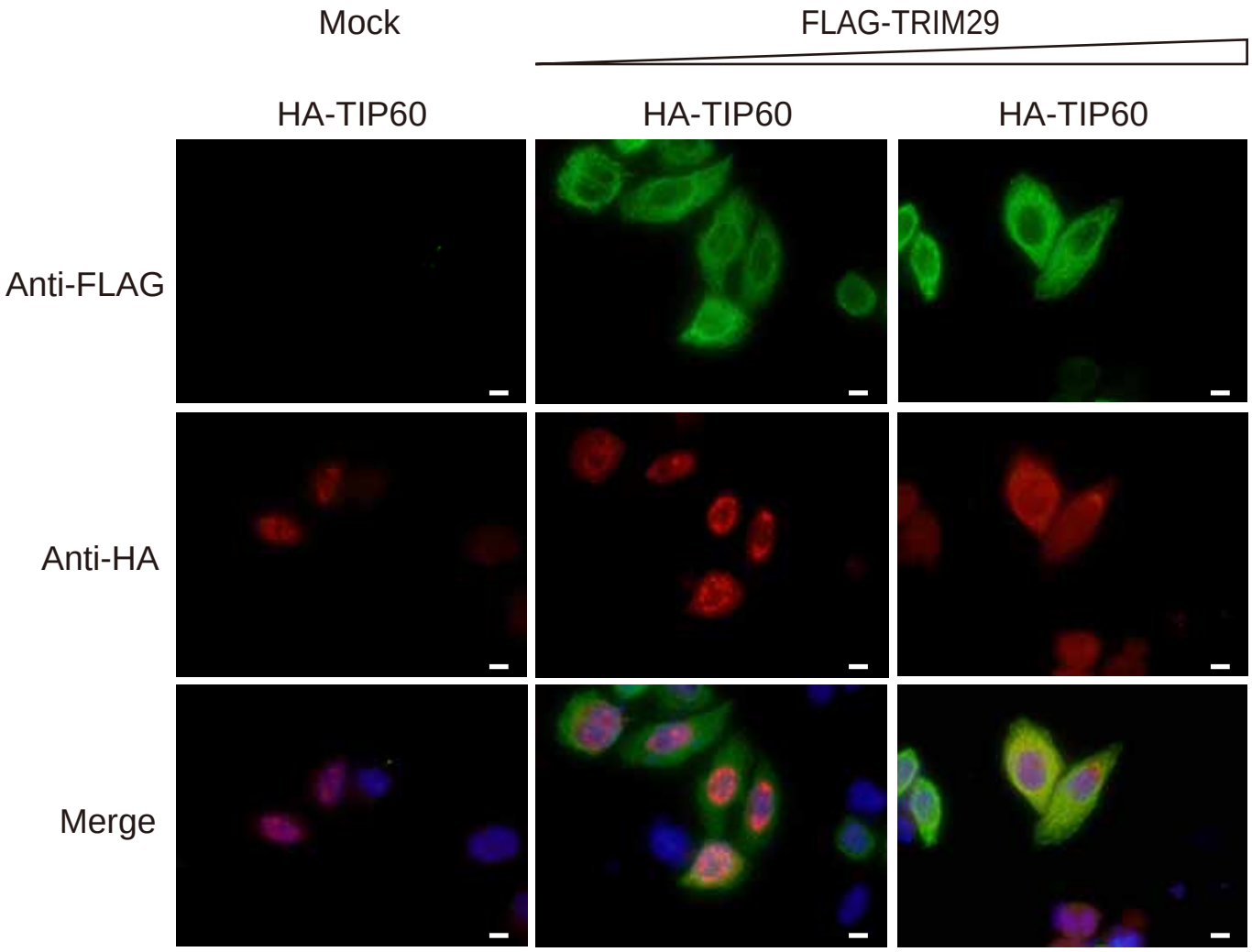

Sho et al. Fig. 2

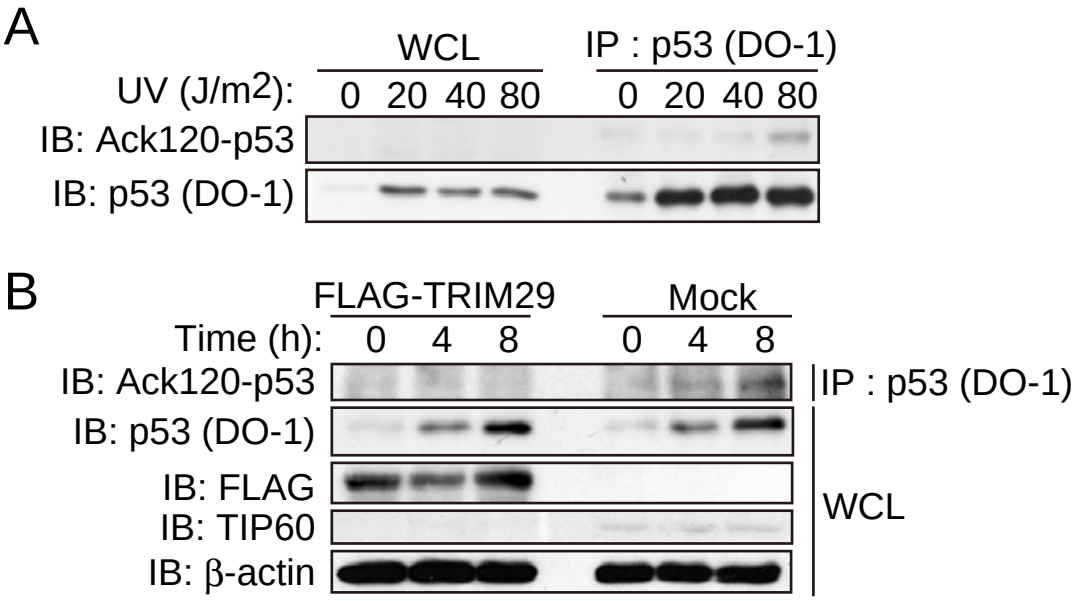

Sho et al. Fig. 3

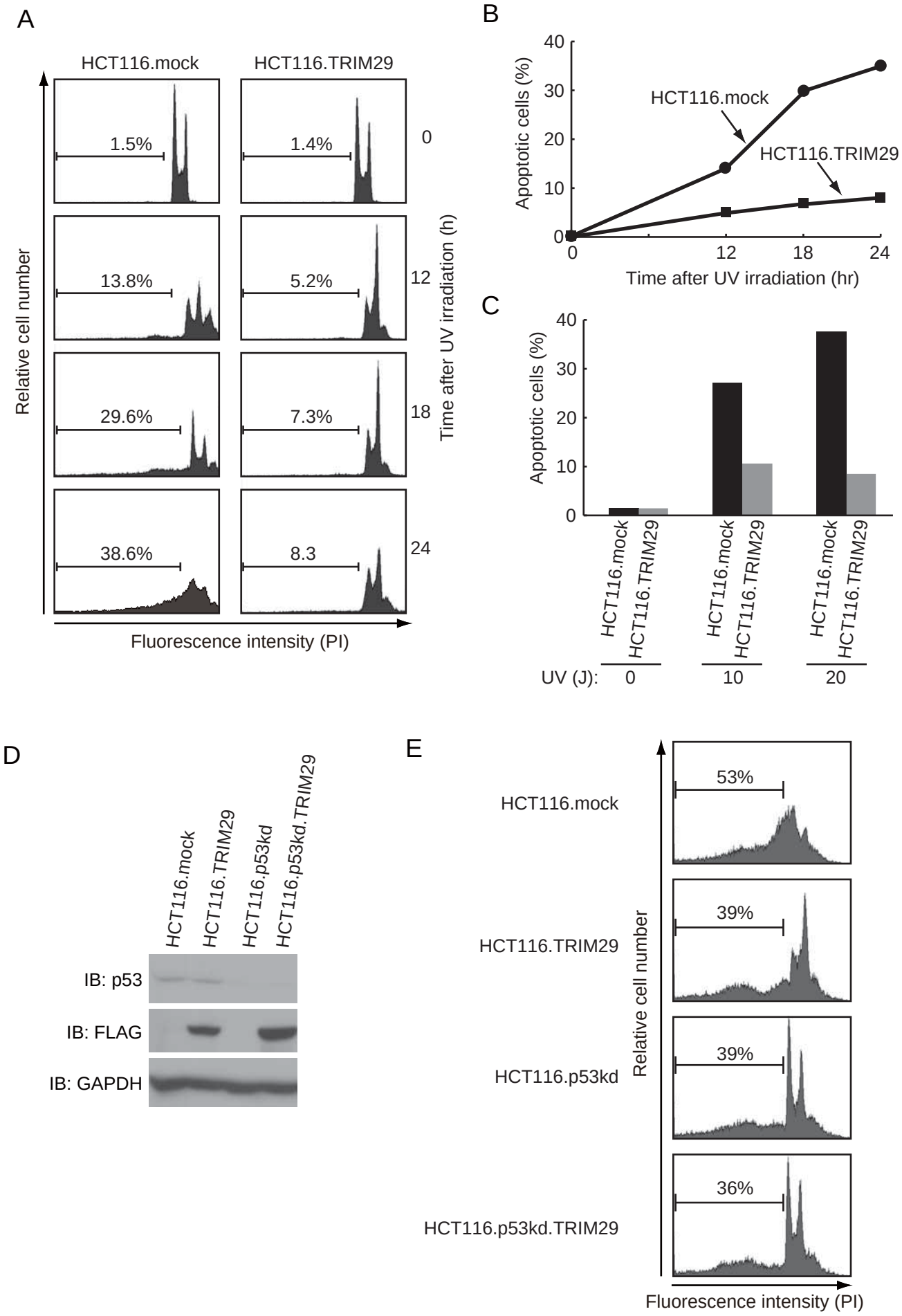

Sho et al. Fig. 4

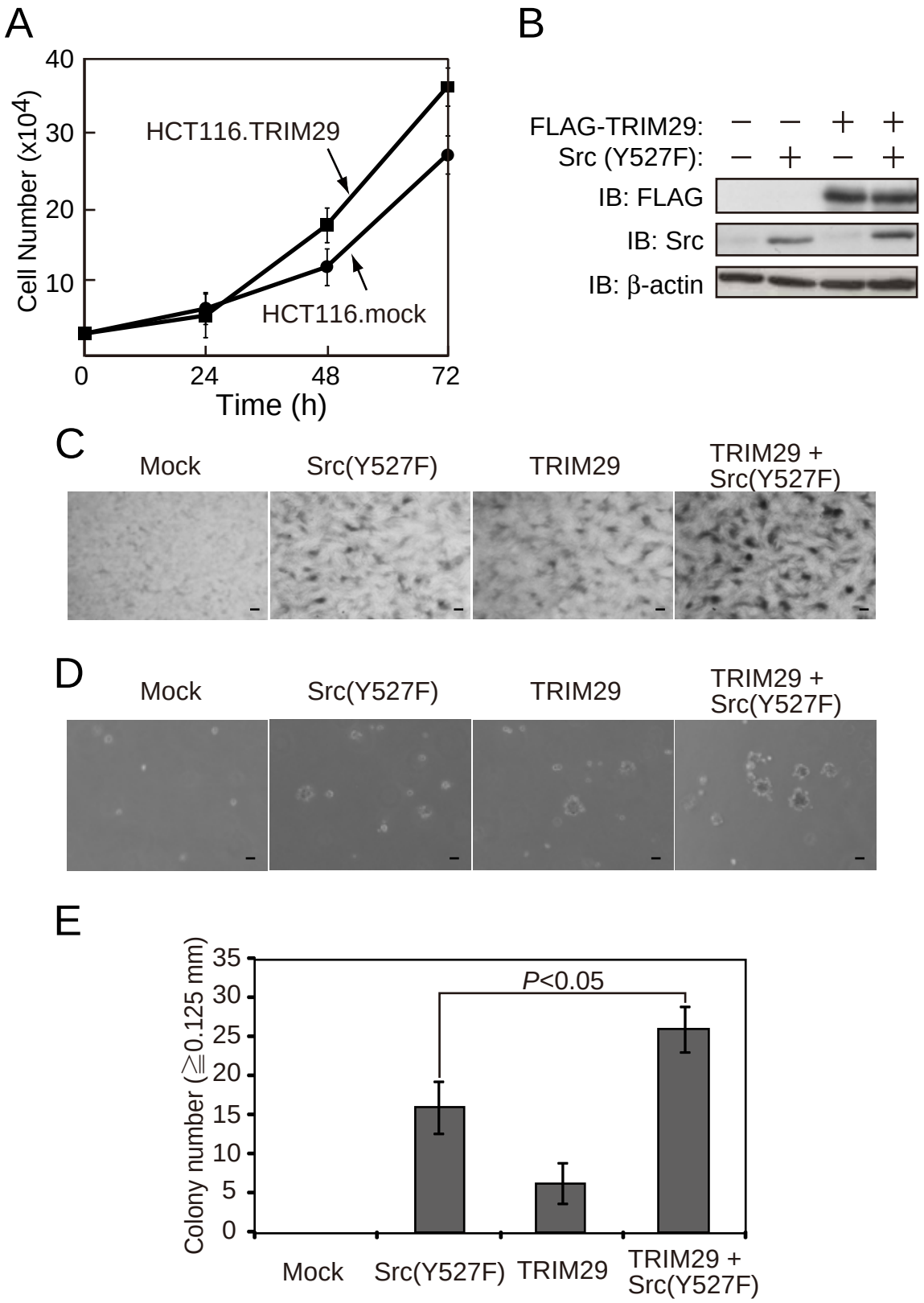

Sho et al. Fig. 5

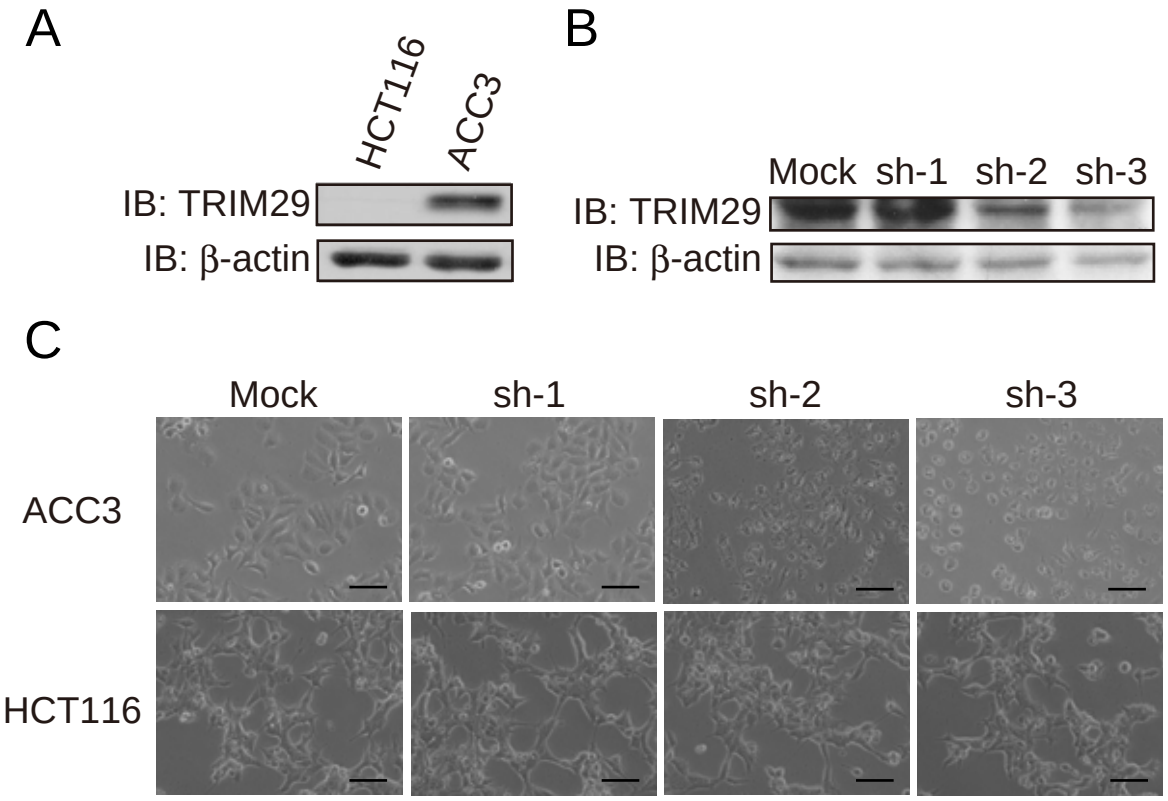

Sho et al. Fig. 6

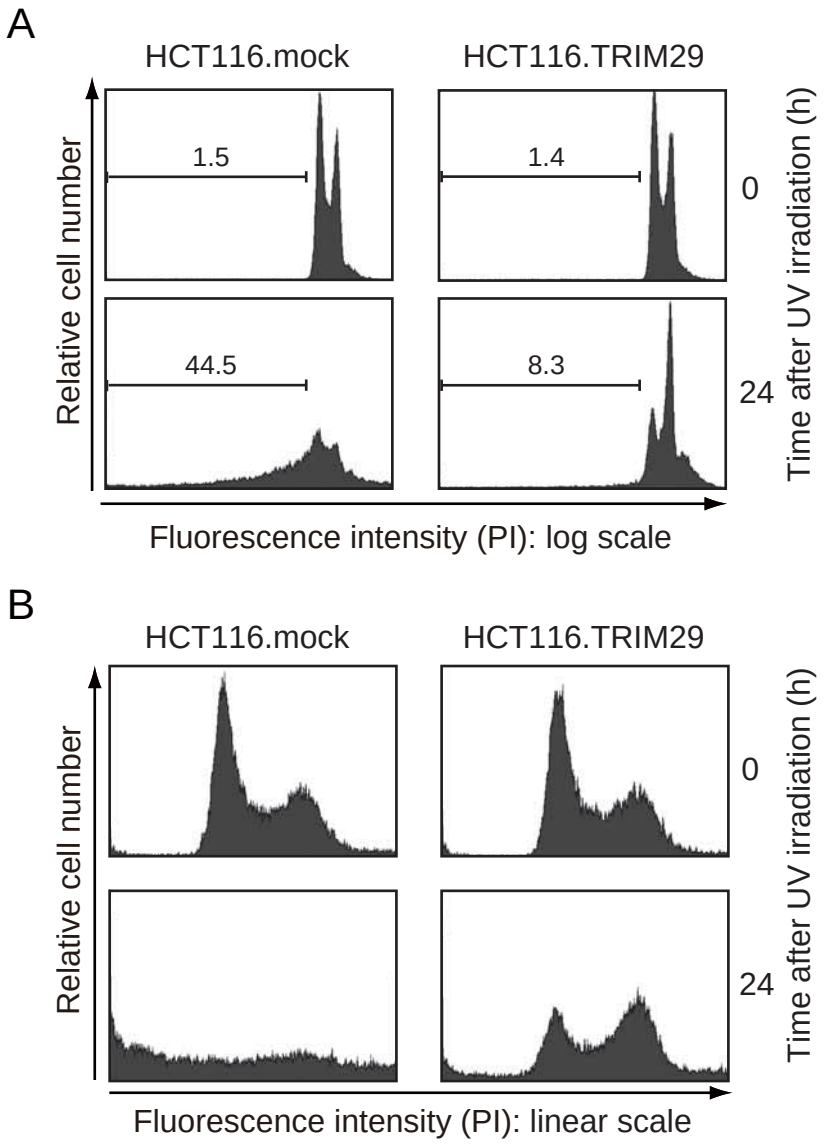

Supplementary Fig. 1. TRIM29 suppresses apoptosis induced by UV treatment. (A) Measurement of sub-G1 peak. HCT116 cell lines were incubated for 0 and 24 h after UV treatment (80 J/m^2). The cells were treated with propidium iodide and then sub-G1 peaks were analyzed with a FACSCalibur flow cytometer in log scale. (B) The data in (A) are shown in linear scale.